Abbas Fattah
Research Scientist
e-mail: fattah@me.udel.edu

Sunil K. Agrawal[1]
Professor
e-mail: agrawal@me.udel.edu

Glenn Catlin

John Hamnett

Mechanical Systems Laboratory,
Department of Mechanical Engineering,
University of Delaware,
Newark, DE 19716

Design of a Passive Gravity-Balanced Assistive Device for Sit-to-Stand Tasks

A sit-to-stand assist device can serve the needs of people suffering from muscle weakness due to age or disabilities that make sit-to-stand a difficult functional task. The objective of this paper is to design a passive gravity-balancing assist device for sit-to-stand motion. In our study, it has been shown that the contribution to the joint torques by the gravitational torque is dominant during sit-to-stand motion. On the basis of this result, a gravity balanced assistive device is proposed. This passive device uses a hybrid method to identify the center-of-mass of the system using auxiliary parallelograms first. Next, appropriate springs are connected to the device to make the total potential energy of the system due to the gravity and the springs constant during standing up. A demonstration prototype with the underlying principles was fabricated to test the feasibility of the proposed design. The prototype showed gravity balancing and was tested by the authors. This prototype will be modified appropriately for clinical testing. [DOI: 10.1115/1.2216732]

1 Introduction

Almost fifty million people in United States are over 65. It is estimated that 18% of this population has limited mobility [1]. As a result, this group needs assistance in activities of daily life. Sit-to-stand (STS) is one of the most common daily activities, which is also a pre-requisite for other functional movements that require ambulation. It is estimated that more than two million people older than 64 years in the United States have difficulty in rising from a chair [2]. STS activity is mechanically demanding [3], where elderly people face difficulty.

Some proposals of assist devices during STS have been reported. Functional electrical stimulation (FES) and/or powered machines have been suggested to augment to the muscle capability [4–7]. Functional electrical stimulation (FES) has been used to help a paraplegic patient to stand up from a wheel chair [4]. Handle reactions have also been used as a measure of stimulation of leg muscles (CHRELMS) during the standing up motion [5]. Kamnik et al. presented a three degrees-of-freedom (3 DOF) robot assistive device to increase the standing up ability in impaired people [6]. Recently, the same authors proposed the integration of standing-up assistive device with FES [8]. The objective of the integration was to build a robot cell to help in multimodal standing-up motion. An assistive robotic device, KineAssist, [7] has been proposed for gait and balance training. The KineAssist provided partial body weight support and postural torques on the torso.

One of the important limitations of these devices is that they are powered and require a support staff for safe operation. The main contribution of this paper is to design a passive gravity-balancing assist device for sit-to-stand motion. Our proposed machine is unpowered and keeps the human body in neutral equilibrium during the entire range of motion. As a result, a subject with this device will be able to stand up from a chair without significant effort. Further, the passive device will minimize risk to the human during use. Such an assist device can be used as (a) a functional rehabilitative aid, (b) a training device, or (c) an evaluation tool for the study of sit-to-stand motion.

A machine is said to be gravity balanced if joint actuator torques are not needed to keep the system in equilibrium in any configuration. Gravity balancing is often used in industrial machines to decrease the required actuator efforts during motion [9–12]. However, this concept has not yet been effectively applied to rehabilitation machines. In recent years, passive gravity balancing orthoses have been proposed for the upper arm [13,12,14]. The authors have proposed designs of passive orthoses to gravity balance human legs during motion [15,16].

In this study, we consider the human body to have three degrees-of-freedom in the sagittal plane during sit-to-stand. In such an activity, the required joint torques are due to gravity, passive muscle forces, and inertia. Since STS movement is relatively slow, the joint torque due to gravity is the most dominant. As a result, we propose a gravity balancing assist device for the STS motion. In order to design gravity balancing for the STS task, it is required to make relevant but simplifying assumptions to come up with an engineering design. STS motion is primarily a planar activity [17] and the gravity balancing is a useful principle that can assist a user in this activity. Our proposed design uses a hybrid method to identify the center-of-mass of the system using auxiliary parallelograms and then attaches appropriate springs to make the total potential energy of the system invariant during the entire motion. A demonstration prototype with the underlying principles was fabricated to test the feasibility of the proposed design for a specific subject.

2 Modeling of the Human Body for STS Task

The human body can be modeled during the sit-to-stand (STS) motion as having three degrees-of-freedom (DOF) [17], as shown in Fig. 1. The sagittal plane approximation holds if both legs do not have any out-of-plane motion. Links $l_s(OO_1)$, $l_t(O_1O_2)$, and $l_H(O_2O_3)$ represent the shank, thigh and HAT (head, arm, and trunk) segments of the human body, respectively. The head, arm and trunk of the body can be considered as a HAT body and its center-of-mass (c.m.) remains fixed during the motion. Note that the mass of HAT is half of the upper body mass. The angles θ_a, θ_k, and θ_h are the ankle, knee, and hip joint angles, respectively.

2.1 Inverse Dynamic Model. The joint torques at the ankle, knee, and hip joints have the following components during mo-

[1]Corresponding author.

Contributed by the Mechanisms and Robotics Committee of ASME for publication in the JOURNAL OF MECHANICAL DESIGN. Manuscript received March 31, 2005; final manuscript received October 10, 2005. Review conducted by Hashem Ashrafiuon. Paper presented at the ASME 2004 Design Engineering Technical Conferences and Computers and Information in Engineering Conference (DETC2004), September 28–October 2, 2004, Salt Lake City, Utah, USA.

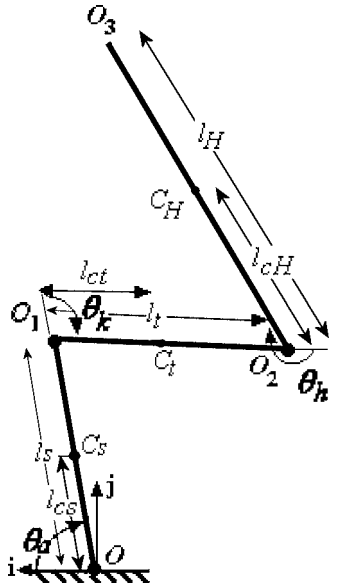

Fig. 1 A 3-DOF planar model of the human body

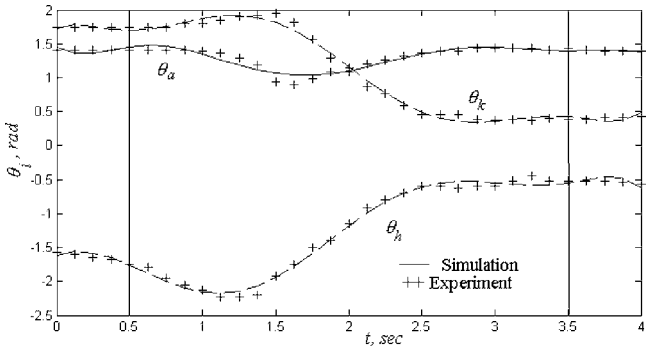

Fig. 2 Joint angles for standing up motion, θ_a (ankle), θ_k (knee), θ_h (hip), from experiment [19] and simulation

$$\theta_a = -0.0080t^7 + 0.1424t^6 - 0.9914t^5 + 3.3609t^4 - 5.6326t^3 + 4.1683t^2 - 1.0681t - 0.1195 \quad (1)$$

$$\theta_k = 0.0094t^7 - 0.1532t^6 + 0.9397t^5 - 2.6138t^4 + 3.0975t^3 - 1.1307t^2 - 0.0885t + 1.7753 \quad (2)$$

$$\theta_h = -0.0030t^7 + 0.0329t^6 - 0.0315t^5 - 0.8191t^4 + 3.6089t^3 - 5.0193t^2 + 1.8540t - 1.6744 \quad (3)$$

These polynomials and the experimental joint angles results given in [19] are shown in Fig. 2. All angles are in radian. Note that the time for STS motion is 4 s for this example. We study the simulation results during 0.5–3.5 s, where the joint accelerations are not too high and the data better matches average human data.

Using Eqs. (1)–(3) and their time derivatives, the inertial and gravitational joint torques are derived using the inverse dynamic model presented in [20]. The passive elastic joint torques due to the muscles can be determined using the exponential relations presented in [19]. The detailed computation of the joint torques are given in the Appendix .

Using Eq. (A3), the inertial, gravitational, passive elastic and total joint torques of ankle, knee, and hip joints are computed and shown in Fig. 3. As shown, the gravitational joint torques are the most dominant. On the basis of this observation, we are encouraged to design a gravity-balanced assistive device such that the gravitational torques of the human body are nearly zero during the STS motion.

tion: (i) An inertial torque due to the inertial forces of the segments, (ii) a passive elastic torque due to stiffness of the muscles, and (iii) a gravitational torque due to gravity. Passive viscous joint torques are of less importance during slow speeds. For a given joint motion, and for known geometric and inertia properties of the segments of the human body, the inertial and gravitational joint torques can be determined using the dynamic model. For example, consider a human body with 1.75 m height and 73 kg weight with the geometric and inertia parameters shown in Table 1. These parameters are for a normal subject and are taken from the Anthropometric Tables [18]. The moment of inertia of each segment is expressed with respect to its center-of-mass. Here, l_{cj} stands for the location of the center-of-mass (c.m.) of the link l_j from its origin.

The time history of the joint angles for the STS motion of a subject can be approximated by the following polynomials [19]:

Table 1 The geometric and inertia parameters for a human body [18]

Link	Dimension (m)	Mass (kg)	c.m. (m)	Moment of inertia (kg m^2)
OO_1, shank	l_s=0.421	3.1	l_{cs}=0.55l_s	I_s=0.0458
O_1O_2, thigh	l_t=0.432	7.39	l_{ct}=0.59l_t	I_t=0.1150
O_2O_3, HAT	l_H=0.8	24.13	l_{cH}=0.41l_H	I_H=1.2869

3 Preliminary Design of the Assistive Device

Our gravity balancing applies to three degrees-of-freedom motion of the body at the hip, knee, and ankle. In our proposed design, the device is to be worn as an orthosis with straps to tie the corresponding moving segments of the machine and the leg. In this design, the following assumptions are made: (i) The motion of

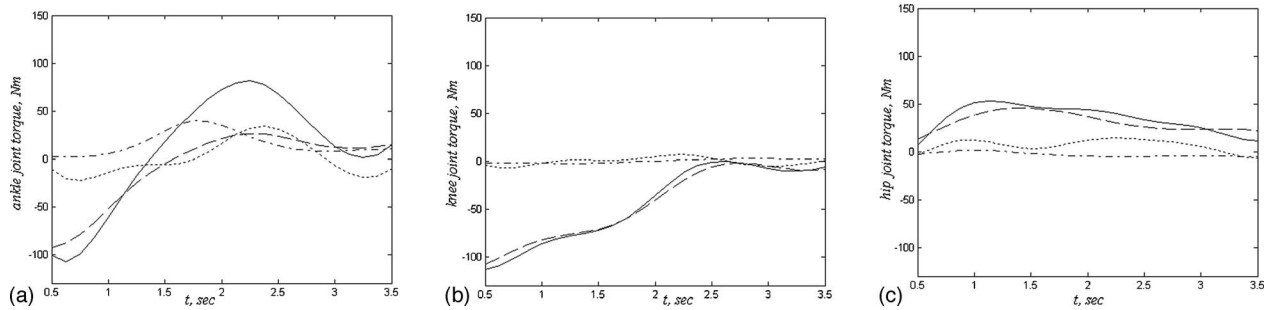

Fig. 3 (*a*) Ankle joint torques, (*b*) knee joint torques, (*c*) hip joint torques. Total: Solid; inertial: Dotted; gravitational: Dashed; and passive: Dashdot

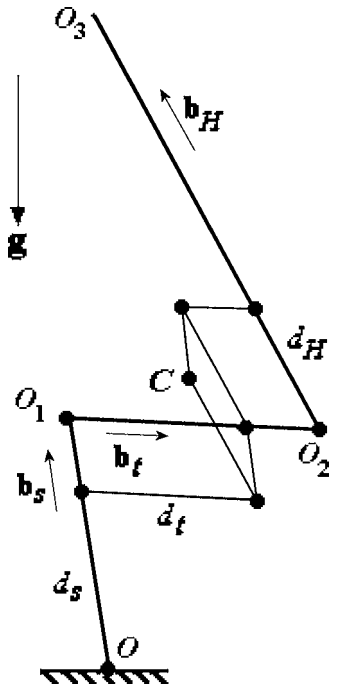

Fig. 4 The 3 DOF human body and device with auxiliary parallelograms to determine the c.m. of the body

the body is in the sagittal plane and both legs have the same motion during the STS motion; (ii) the device links are lightweight and do not add significant mass to the moving limbs, once strapped to the subject's body; (iii) the c.m. of each link is assumed to lie on the line connecting the two joints.

To make a gravity-balanced assistive device for the human body, the following procedure is used: (i) Determine the c.m. of the system, i.e., device and the human body using auxiliary parallelograms; (ii) select springs to connect to the system c.m. such that the total potential energy of the system is invariant with configuration. This hybrid method allows one to physically determine the system c.m. and connect this point to the inertially fixed frame through springs [12].

3.1 Locating the Center-of-Mass using Auxiliary Parallelograms. The location of c.m. for the three-link of the human body shown in Fig. 4 from the point O is defined by $\mathbf{r}_{OC}$. Its expression is given by

$$\mathbf{r}_{OC} = d_s\mathbf{b}_s + d_t\mathbf{b}_t + d_H\mathbf{b}_H$$

where

$$d_s = \frac{1}{M}(m_t l_s + m_H l_s + m_s l_{cs})$$

$$d_t = \frac{1}{M}(m_H l_t + m_t l_{ct})$$

$$d_H = \frac{1}{M} m_H l_{cH} \tag{4}$$

and

$$M = m_s + m_t + m_H \tag{5}$$

Here, $\mathbf{b}_j$ is the unit vector along link l_j, m_s, m_t, and m_H are the masses of shank, thigh, and HAT, respectively, M is half of the total mass of the body. Note that d_j are factors of geometry and mass distribution of the links and are usually denoted by the terminology "scaled lengths." The three scaled lengths can then be used to form parallelograms in order to identify the c.m. C shown in Fig. 4 [12]. The system consists of parallelograms in two layers, the first layer has two parallelograms while the second layer has one.

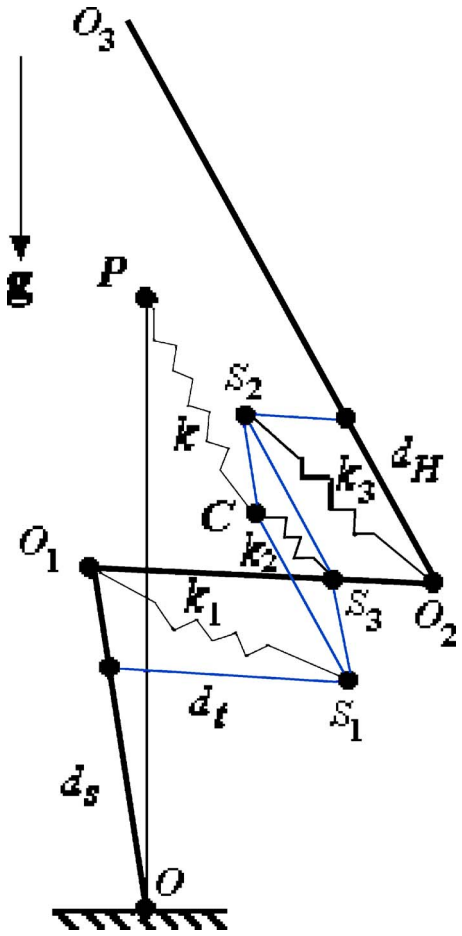

Fig. 5 Spring attachments of the 3 DOF human body

3.2 Spring Selections. The human body and the device can be gravity-balanced by attaching four springs to the system as shown in Fig. 5. The total potential energy of the system consists of gravitational and elastic energies due to the springs. Its expression is given by

$$V = V_s + V_g \tag{6}$$

$$= \tfrac{1}{2}kx^2 + \tfrac{1}{2}k_1x_1^2 + \tfrac{1}{2}k_2x_2^2 + \tfrac{1}{2}k_3x_3^2 - M\mathbf{g}\cdot\mathbf{r}_{\mathbf{OC}} \tag{7}$$

Upon substitution of the $x^2 = \|\mathbf{PC}\|\cdot\|\mathbf{PC}\|$, $x_1^2 = \|\mathbf{O_1S_1}\|\cdot\|\mathbf{O_1S_1}\|$, $x_2^2 = \|\mathbf{CS_3}\|\cdot\|\mathbf{CS_3}\|$ and $x_3^2 = \|\mathbf{O_2S_2}\|\cdot\|\mathbf{O_2S_2}\|$ and expanding the results thus obtained in terms of joint angles, one obtains

$$-M\mathbf{g}\cdot\mathbf{r}_{\mathbf{OC}} = Mg(d_s s_a + d_t s_{ak} + d_H s_{akh}) \tag{8}$$

$$x^2 = (d_s c_a + d_t c_{ak} + d_H c_{akh})^2 + (d_s s_a + d_t s_{ak} + d_H s_{akh} - d)^2 \tag{9}$$

$$x_1^2 = d_t^2 + (l_s - d_s)^2 - 2(l_s - d_s)d_t c_k \tag{10}$$

$$x_2^2 = d_H^2 + (l_s - d_s)^2 - 2d_H(l_s - d_s)c_{kh} \tag{11}$$

$$x_3^2 = (l_t - d_t)^2 + d_H^2 - 2d_H(l_t - d_t)c_h \tag{12}$$

Here, c_i, s_i, c_{ij}, s_{ij}, c_{ijk}, and s_{ijk} stand for $\cos\theta_i$, $\sin\theta_i$, $\cos(\theta_i + \theta_j)$, $\sin(\theta_i + \theta_j)$, $\cos(\theta_i + \theta_j + \theta_k)$, and $\sin(\theta_i + \theta_j + \theta_k)$, respectively. $d = \|\mathbf{OP}\|$ is the distance along the gravity vector as shown in Fig.

5. Also, x and x_i are deformation and k and k_i, $i=1,2,3$ are stiffness of the springs. In this analysis, it is assumed that the undeformed length of the spring is zero. In other words, the spring force is zero when the length of the spring is also zero. In the physical implementation of zero free length, nonzero free length spring can be used behind the pulley where the spring force can be transmitted through the string. Upon substitution of Eqs. (8)–(12) into Eq. (7), one obtains

$$V = \tfrac{1}{2}k(d_s^2 + d_t^2 + d_H^2 + 2d_s d_t c_k + 2d_s d_H c_{kH} + 2d_t d_H c_h - 2d_s ds_a - 2d_t ds_{ak} - 2d_h ds_{akh}) + \tfrac{1}{2}k_1(d_t^2 + (l_s - d_s)^2 - 2(l_s - d_s)d_t c_k) + \tfrac{1}{2}k_2(d_H^2 + (l_s - d_s)^2 - 2d_H(l_s - d_s)c_{kh}) + \tfrac{1}{2}k_3((l_t - d_t)^2 + d_H^2 - 2d_H(l_t - d_t)c_h) + Mg(d_s s_a + d_t s_{ak} + d_H s_{akh}) \quad (13)$$

Equation (13) can be rearranged in terms of configuration variables as

$$V = C_V + [kd_s - k_1(l_s - d_s)]d_t c_k + [kd_s - k_2(l_s - d_s)]d_H c_{kh} + [kd_t - k_3(l_t - d_t)]d_H c_h + (Mg - kd)(d_s s_a + d_t s_{ak} + d_H s_{akh}) \quad (14)$$

where

$$C_V = \tfrac{1}{2}k(d_s^2 + d_t^2 + d_H^2) + \tfrac{1}{2}k_1(d_t^2 + (l_s - d_s)^2) + \tfrac{1}{2}k_2(d_H^2 + (l_s - d_s)^2) + \tfrac{1}{2}k_3((l_t - d_t)^2 + d_H^2) \quad (15)$$

On setting the coefficients of the configuration variables in Eq. (14) to zero, the desired stiffness of the springs for gravity balancing of the system are derived as

$$k = \frac{Mg}{d}$$

$$k_1 = \frac{kd_s}{l_s - d_s}$$

$$k_2 = \frac{kd_s}{l_s - d_s}$$

$$k_3 = \frac{kd_t}{l_t - d_t} \quad (16)$$

The connection points of springs k_1 and k_2 are chosen such that $k_1 = k_2$. However, in general, k_1 and k_2 are different. More details of the computations are available in [15].

3.3 Numerical Example. As an example, the geometric and inertia parameters in Table 1 are used to design a gravity-balanced assistive device. To this end, inserting these parameters into Eqs. (4) and the result thus obtained into Eqs. (16), we obtain, $d_s = 0.404$ m, $d_t = 0.355$ m, $d_H = 0.231$ m, $k = 0.34/d$ kN/m, $k_1 = k_2 = 8.3/d$ kN/m, $k_3 = 1.58/d$ kN/m. Note that d is an adjustable distance. Using Eqs. (16), it is easy to show that by increasing the distance d, the stiffness of spring k decreases and thus the stiffness of springs k_1, k_2, and k_3 decrease likewise. However, the extension of spring k is related to the difference between the vertical distance of system c.m. and d, see Eq. (9). As a result the variable d is chosen such that we have optimal values for the stiffness of the springs and the extension of the spring k. In this example, the distance is chosen as $d = 0.75$ m.

Consider the joint motion given in Eqs. (1)–(3). The joint torques for this example and the above mentioned motion can be obtained using the model explained in Sec. 2.1 without considering the gravitational forces. The joint torques for both cases (i) the normal human body (solid line) and (ii) the human body with gravity balancing assistive device (dashed line) are shown in Fig. 6. Here, τ_a, τ_k, and τ_h are ankle, knee, and hip torques, respectively. As shown, the joint torques are reduced substantially for the human body using the assistive device.

Please note that the effect of leg mass is important in gravity balancing during the STS task. The leg mass is about 40% of the HAT mass and affects the gravity balancing of the human body.

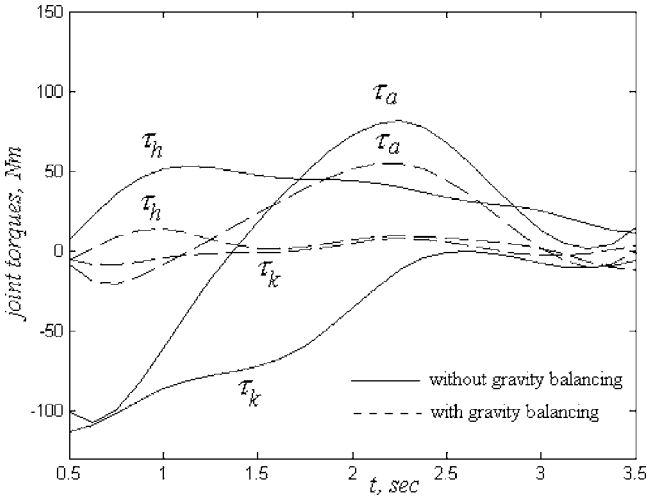

Fig. 6 Joint torques with gravity balancing and without gravity balancing

4 Preliminary Design Problems

The preliminary design brought out some interesting engineering questions which are worth pointing out: (i) Since the springs should compensate for the weight of whole body, the stiffness of the springs are high; (ii) the size of the auxiliary parallelograms are small and it is difficult to physically fabricate them.

For example, the stiffness of the springs for the preliminary design in Sec. 3.3, with the parameters given in Table 1 are as follows:

$$k = 0.45 \text{ kN/m}$$

$$k_1 = 11.04 \text{ kN/m}$$

$$k_2 = k_1$$

$$k_3 = 2.1 \text{ kN/m} \quad (17)$$

Using Fig. 5, the extension for each spring can be written in terms of joint angles as $\|PC\| = x$, $\|O_1S_1\| = x_1$, $\|CS_3\| = x_2$, and $\|O_2S_2\| = x_3$, where x and x_i, $i=1,2,3$ are given in Eqs. (9)–(12).

The force of each spring can be obtained by multiplying the stiffness of each spring by its extension as follows:

$$f_{PC} = kx$$

$$f_{O_1S_1} = k_1 x_1$$

$$f_{CS_3} = k_2 x_2$$

$$f_{O_2S_2} = k_3 x_3 \quad (18)$$

The spring extensions and spring forces for the above example during the STS motion of Fig. 2 are shown in Fig. 7 using the above relations. As shown, the springs have large extensions and also have high stiffness. This results in the exertion of large forces on the device. Further, it is hard to find springs with both large extension and high stiffness.

To alleviate these problems, the design is modified to have a smaller stiffness of the springs and a larger size for the auxiliary linkages. This is achieved by using the following key ideas: (a) Use an ankle weight leading to a larger size for the parallelograms; (b) use a body weight support (harness) to partially reduce the weight of the body; (c) alter the location of the center-of-mass to reduce the stiffness of the springs. The stiffness of the springs is

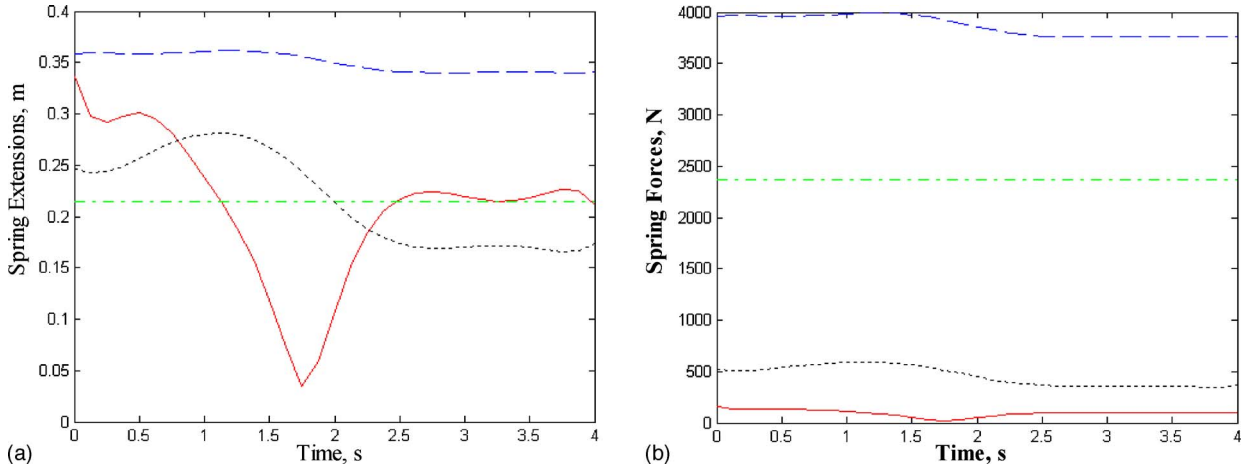

Fig. 7 Spring extensions (*a*) and spring forces (*b*) for the preliminary design. x and f_{PC}: Solid line; x_1 and $f_{O_1S_1}$: Dashed; x_2 and f_{S_3C}: Dashdot; x_3 and $f_{O_2S_2}$: Dotted.

a function of the total weight of the system and the scaled lengths d_s, d_t, and d_H. The total weight of the system can be reduced by the body weight support **W**. Also, the scaled lengths increase by adding ankle weight $\mathbf{m_e}$ at each leg. To have reasonable stiffness and extensions for the springs, we chose an appropriate ankle weight at each leg and body weight support which connects to c.m. of HAT(upper body) to reduce the stiffness of the springs as shown in Fig. 8. As an example, the stiffness of the springs for $\mathbf{m_e}=3$ kg and $\mathbf{W}=23$ kg are given as

$$k = 0.34 \text{ kN/m}$$

$$k_1 = 1.91 \text{ kN/m}$$

$$k_2 = k_1$$

$$k_3 = 0.6 \text{ kN/m} \tag{19}$$

The extension and force of the springs for the new design is shown in Fig. 9. Upon comparison of Figs. 7 and 9, one can infer that the spring extensions and forces in new design are much smaller than the preliminary one. Furthermore, the size of the auxiliary parallelograms are larger for the new design as shown in Fig. 10. Nevertheless, if it is not desired to have body support for this device, it is possible to use the first method to reduce the stiffness of the springs without using body support. By added mass at the ankle joints, it is possible to have springs with reasonable stiffness. This increases the size of the auxiliary parallelograms. Lightweight materials for assistive device can be used to keep the weight to a minimum.

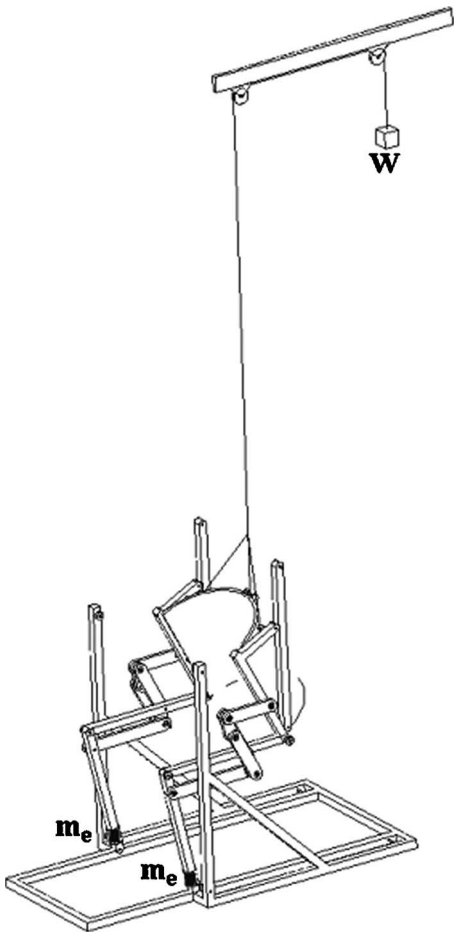

Fig. 8 Schematic model of the new design

5 Demonstration Prototype

A demonstration prototype was fabricated based on the feedback from the preliminary design at University of Delaware and is shown in Fig. 11. The engineering prototype includes the following features: (i) All segments of the prototype are made of extruded aluminum. This allows for easy adjustment of the device, have revolute joints with minimal friction, and an overall lightweight design; (ii) the design is modified to have smaller stiffness of the springs and larger size for auxiliary linkages; (iii) the springs are rigidly attached to the extruded aluminum and fit through a network of pulleys and cables to have zero free-length spring; (iv) the leg straps are riveted to the extruded aluminum and use a tightening hook to make a firm attachment to the human subject. The back brace is fitted to the lower back with aluminum covered by leather, there is also a corset front that buckles up around the front of a patient. This back brace is then rigidly attached to the extruded aluminum. This attachment allows for the assumption that the head, arms, and trunk of a patient is evenly distributed to the main links on either side of the patient; (v) the links of the device are lightweight and do not add significant mass to the moving limbs, once strapped to a subject's leg; (vi) the two separate sides are connected by the back brace and the corset through the HAT as shown in Fig. 8.

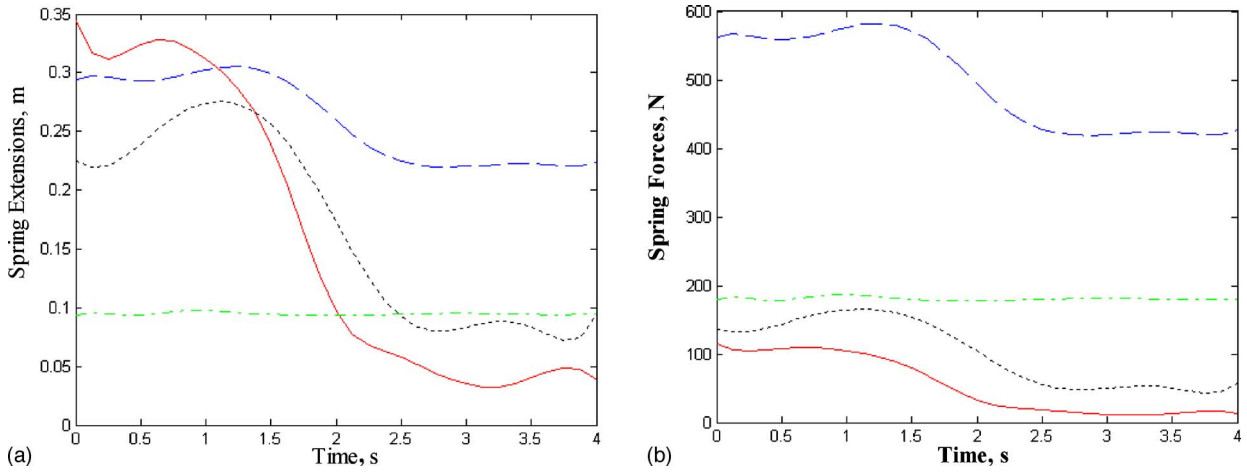

Fig. 9 Spring extensions (*a*) and spring forces (*b*) for the new design. x and f_{PC}: Solid line; x_1 and $f_{O_1S_1}$: Dashed; x_2 and f_{S_3C}: Dashdot; x_3 and $f_{O_2S_2}$: Dotted.

Even though no quantitative data is presented in the paper, the prototype verifies the concept of gravity balancing when tested by the authors. A representative photograph is shown in Fig. 12.

This device can be validated by collecting movement and electromyograph (EMG) data from users in the device. EMG activity can be recorded from muscles that are involved in moving the limb into the desired positions. Lumbar paraspinal, quadriceps, and hamstrings are activated in a consistent patterned sequence during the STS motion [21] and thus can be considered for EMG data collection. Data can be collected when both the assistive device is attached to the user and when it is not attached to the user to confirm that the assistive device reduces the muscle activities during the STS motion. The authors have already been involved in EMG data collection for a gravity balancing leg orthosis for robotic rehabilitation [22].

This prototype was designed to only demonstrate the overall concept and it will be modified appropriately for clinical testing. In further developments of the prototype, we plan to introduce the following additional features: (i) Segments will be made to be telescopic to accommodate variability in the leg dimensions and inertia across human subjects; (ii) safe and simple patient/machine interface; (iii) ease of STS transfer, safety, and comfort with the proposed device; and (iv) the use of joint position and force/torque sensors to monitor the kinematics and kinetics of human/machine limbs.

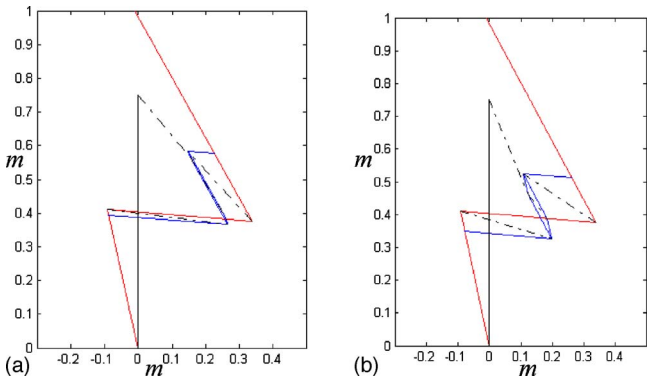

Fig. 10 (*a*) Auxiliary parallelograms for the preliminary design, (*b*) auxiliary parallelograms for the new design

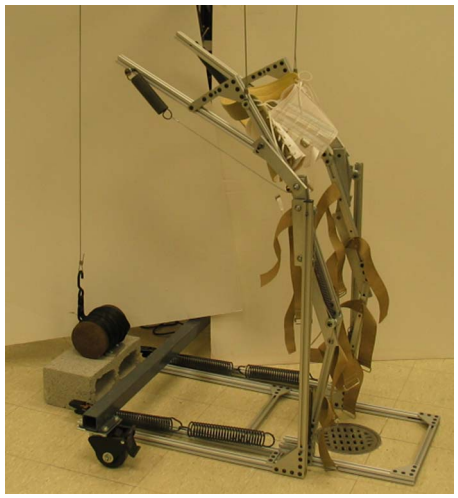

Fig. 11 Photograph of the new prototype of the assistive design

6 Conclusions

We proposed a passive gravity-balanced device to assist the patients during the sit-to-stand task. A hybrid method was used to locate the system center-of-mass and then attach suitable springs to make the total potential energy of the system invariant with configuration. Based on these results, an engineering prototype was fabricated. This prototype shows that this conceptual idea of gravity balancing can be applied for the sit-to-stand task. Future research work will address the problem of a quantitative evalua-

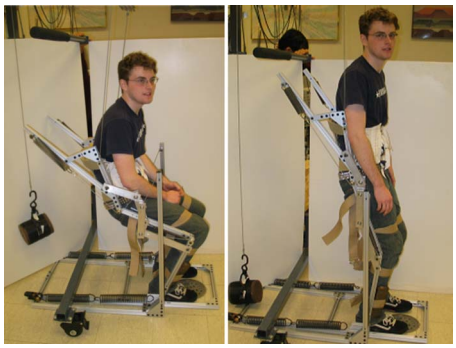

Fig. 12 Photographs of the new prototype with the subject in sit and stand positions

tion of the device, using electromyograph data of the muscles involved in the motion of the leg, safe and simple patient/machine interface, and accommodate variability in geometry and inertia of subjects.

Acknowledgment

The support of NIH Grant No. 1RO1 HD38582-01A2 is gratefully acknowledged.

Nomenclature

c.m. = center-of-mass
HAT = head, arm, and trunk
θ_a = ankle joint angle
θ_k = knee joint angle
θ_h = hip joint angle
l_s = shank segment
l_t = thigh segment
l_H = HAT segment
l_{cs} = shank c.m. from its origin
l_{ct} = thigh c.m. from its origin
l_{cH} = HAT c.m. from its origin
τ_a = ankle joint torque
τ_k = knee joint torque
τ_h = hip joint torque
τ_{ad} = inertial ankle joint torque
τ_{kd} = inertial knee joint torque
τ_{hd} = inertial hip joint torque
τ_{ag} = gravitational ankle joint torque
τ_{kg} = gravitational knee joint torque
τ_{hg} = gravitational hip joint torque
τ_{ae} = passive elastic ankle joint torque
τ_{ke} = passive elastic knee joint torque
τ_{he} = passive elastic hip joint torque
$\mathbf{r}_{OC}$ = system c.m.
$\mathbf{b}_j$ = unit vector along link l_j
d_j = scaled length of link l_j
M = half of the total mass of the human body
m_s = shank mass
m_t = thigh mass
m_H = HAT mass
V = total potential energy of the system
V_g = gravitational potential energy
V_s = elastic energy due to the springs
k_j = stiffness of spring j
x_j = deformation of spring j
c_i = cos θ_i
s_i = sin θ_i
c_{ijk} = cos$(\theta_i+\theta_j+\theta_k)$
s_{ijk} = sin$(\theta_i+\theta_j+\theta_k)$
$\mathbf{g}$ = gravity vector
d = distance along the gravity vector
f_{ij} = force of spring between i to j
$\mathbf{W}$ = body weight support
$\mathbf{m}_e$ = ankle weight
I_{ij} = elements of inertia matrix

Appendix

The joint torques at the ankle, knee, and hip joints consist of inertial, passive elastic, and gravitational torques can be written as

$$\tau_a = \tau_{ad} + \tau_{ag} + \tau_{ae} \tag{A1}$$

$$\tau_k = \tau_{kd} + \tau_{kg} + \tau_{ke} \tag{A2}$$

$$\tau_h = \tau_{hd} + \tau_{hg} + \tau_{he} \tag{A3}$$

where τ_{ag}, τ_{kg}, and τ_{hg} are ankle, knee, and hip gravitational torques, and τ_{ad}, τ_{kd}, and τ_{hd} are ankle, knee, and hip inertial torques, respectively, while τ_{ae}, τ_{ke}, and τ_{he} are ankle, knee, and hip passive elastic torques, respectively.

The inertial and gravitational joint torques are derived using the inverse dynamic model presented in [20] as

$$\tau_{ag} = m_s g l_{cs} c_a + m_t g (l_s c_a + l_{ct} c_{ak}) + m_H g (l_s c_a + l_t c_{ak} + l_{cH} c_{akh})$$

$$\tau_{kg} = m_t g l_{ct} c_{ak} + m_H g (l_t c_{ak} + l_{cH} c_{akh})$$

$$\tau_{hg} = m_H g l_{cH} c_{akh}$$

$$\tau_{ad} = I_{11}\ddot{\theta}_a + I_{12}\ddot{\theta}_k + I_{13}\ddot{\theta}_h + f_1$$

$$\tau_{kd} = I_{12}\ddot{\theta}_a + I_{22}\ddot{\theta}_k + I_{23}\ddot{\theta}_h + f_2 - \frac{\gamma_2}{2}$$

$$\tau_{hd} = I_{13}\ddot{\theta}_a + I_{23}\ddot{\theta}_k + I_{33}\ddot{\theta}_h + f_3 - \frac{\gamma_3}{2} \tag{A4}$$

where I_{ij}, the elements of inertia matrix, are

$$I_{11} = I_s + I_t + I_H + m_s l_{cs}^2 + m_t (l_s^2 + l_{ct}^2 + l_s l_t c_k) + m_H (l_s^2 + l_t^2 + l_{cH}^2 + 2 l_s l_t c_k + l_s l_H c_{kh} + l_t l_H c_h)$$

$$I_{12} = I_t + I_H + (m_t (2 l_{ct}^2 + l_s l_t c_k) + m_H (2 l_t^2 + 2 l_{cH}^2 + 2 l_s l_t c_k + l_s l_H c_{kh} + 2 l_t l_H c_h))/2$$

$$I_{13} = I_H + m_H (2 l_{cH}^2 + l_s l_H c_{kh} + l_t l_H c_h)/2$$

$$I_{22} = I_t + I_H + m_t l_{ct}^2 + m_H (l_{ct}^2 + l_{cH}^2 + l_t l_H c_h)$$

$$I_{23} = I_H + m_H (l_H^2/2 + l_t l_H c_h)/2$$

$$I_{33} = I_H + m_H l_{cH}^2 \tag{A5}$$

and f_i and γ_i are centrifugal and Coriolis terms as

$$\gamma_2 = -(m_t l_s l_t s_k + m_H (2 l_s l_t s_k + l_s l_H s_{kh}))\dot{\theta}_a^2 - (m_t l_s l_t s_k + m_H (2 l_s l_t s_k + l_s l_H s_{kh}))\dot{\theta}_a \dot{\theta}_k - m_H l_s l_H s_{kh} \dot{\theta}_a \dot{\theta}_h$$

$$\gamma_3 = -m_H (l_s l_H s_{kh} + l_t l_H s_h)\dot{\theta}_a^2 - m_H (l_s l_H s_{kh} + 2 l_t l_H s_h)\dot{\theta}_a \dot{\theta}_k - m_H (l_s l_H s_{kh} + l_t l_H s_h)\dot{\theta}_a \dot{\theta}_h - m_H l_t l_H s_h \dot{\theta}_h^2 - m_H l_t l_H s_h \dot{\theta}_a \dot{\theta}_h$$

$$f_1 = -(m_t l_s l_t s_k + m_H l_s (2 l_t s_k + l_H s_{kh}))\dot{\theta}_a \dot{\theta}_k - m_H l_H (l_s s_{kh} + l_t s h)\dot{\theta}_a \dot{\theta}_h - (m_t l_s l_t s_k + m_H l_s (2 l_t s_k + l_H s_{kh}))\frac{\dot{\theta}_a^2}{2} - m_H l_H (l_s s_{kh} + l_t s h)\dot{\theta}_k \dot{\theta}_h - m_H l_H (l_s s_{kh} + l_t s_h)\frac{\dot{\theta}_h^2}{2}$$

$$f_2 = -(m_t l_s l_t s_k + m_H l_s (2 l_t s_k + l_H s_{kh}))\frac{\dot{\theta}_a \dot{\theta}_k}{2} - m_H l_H (l_s s_{kh} + l_t s_h)\frac{\dot{\theta}_a \dot{\theta}_h}{2} - m_H l_t l_H s_h \dot{\theta}_k \dot{\theta}_h - mHltlHs_h \frac{\dot{\theta}_h^2}{2}$$

$$f_3 = -m_H l_s l_H s_{kh}\frac{\dot{\theta}_a \dot{\theta}_h}{2} - m_H l_H (l_s s_{kh} + l_t s_h)\frac{\dot{\theta}_a \dot{\theta}_h}{2} - m_H l_t l_H \frac{\dot{\theta}_k \dot{\theta}_h}{2} \tag{A6}$$

All parameters are defined in Sec. 2.1.

The passive elastic joint torques due to the muscles can be determined using the exponential relations presented in [19] as

$$\tau_{ae} = \exp(2.0111 - 0.0833(\theta_a - 90) - 0.0090\theta_k) - \exp(-9.9250 + 0.2132(\theta_a - 90)) - 2.970$$

$$\tau_{ke} = \exp(1.0372 + 0.0040(\theta_a - 90) - 0.0494\theta_k - 0.025\theta_h) - \exp(-1.1561 - 0.0020(\theta_a - 90) + 0.0254\theta_k + 0.0030\theta_h) + \exp(2.5 - 0.25\theta_k) + 1$$

$$\tau_{he} = \exp(2.1080 - 0.0160\theta_k - 0.0195\theta_h) - \exp(-2.1784 + 0.070\theta_k + 0.1349\theta_h) - 15.24 \quad \text{(A7)}$$

Here, all joint angles are in degrees.

References

[1] Ficke, R. C., 1991, "Digest of Data on Persons with Disabilities," Technical report, *National Institute on Disabilities and Rehabilitation Research*, Washington, DC.

[2] Dawson, D., Hendershot, G., and Fulton, J., 1987, "Aging in the Eighties: Functional Limitations of Individuals Age 65 and Over," *National Center for Health Statistics Advance Data*, U.S. Department of Health and Human Services, 133, pp. 1–11.

[3] Riley, P. O., Schnekman, M. L., et al., 1991, "Mechanics of a Constrained Chair-Rise," J. Biomech., **24**(1), pp. 77–85.

[4] Bajd, T., Karl, J., and Turk, R., 1982, "Standing-Up of a Healthy Subject and a Paraplegic Patient," J. Biomech., **15**(1), pp. 1–10.

[5] Donaldson, N. de N., and Yu, C.-H., 1996, "FES Standing: Control by Handle Reactions of Leg Muscle Stimulation (CHRELMS)," IEEE Trans. Rehabil. Eng., **4**(4), pp. 280–284.

[6] Kamnik, R., and Bajd, T., 2003, Robot Assistive Device for Augmenting Standing-Up Capabilities in Impaired People," *Proceedings of the 2003 IEEE/RSJ Int. Conference on Intelligent Robot and Systems*, pp. 3606–3611, Las Vegas, Nevada.

[7] Peshkin, M., et al., 2005, "KineAssist: A Robotic Overground Gait and Balance Training Device," *Proceedings of the 2005 IEEE 9th Int. Conference on Rehabilitation Robotics*, pp. 241–246, Chicago, IL.

[8] Kamnik, R., Bajd, T., et al., 2005, "Rehabilitation Robot Cell for Multimodal Standing-Up Motion Augmentation," *Proceedings of the 2005 IEEE Int. Conference on Robotics and Automation*, pp. 2289–2294, Barcelona, Spain.

[9] Streit, D. A., and Shin, E., 1993, "Equilibrators for Planar Linkages," ASME J. Mech. Des., **115**(3), pp. 604–610.

[10] Rahman, T., Ramanathan, R., Seliktar, R., and Harwin, W., 1995, "A Simple Technique to Passively Gravity-Balance Articulated Mechanisms," ASME J. Mech. Des., **117**, pp. 655–658.

[11] Ebert-Uphoff, I., Gosselin, C. M., and Laliberte, T., 2000, "Static Balancing of Spatial Parallel Platform Mechanisms-Revisited," ASME J. Mech. Des., **122**(1), pp. 43–51.

[12] Agrawal, S. K., Gardner, G., and Pledgie, S., 2001, "Design and Fabrication of a Gravity Balanced Planar Mechanism Using Auxiliary Parallelograms," ASME J. Mech. Des., **123**(4), pp. 525–528.

[13] Rahman, T., Sample, W., Seliktar, R., Alexander, M., and Scavina, M., 2000, "A body-powered functional upper limb orthosis," J. Rehabil. Res. Dev., **37**(6), pp. 675–680.

[14] Cardoso, L. F., Tomazio, S., and Herder, J. L., 2002, "Conceptual Design of a Passive Arm Orthosis," in *Proceedings, ASME Design Engineering Technical Conferences*, Paper No. MECH-34285, Montreal, Canada.

[15] Agrawal, S. K., and Fattah, A., 2004, "Theory and Design of an Orthotic Device for Full or Partial Gravity-Balancing of a Human Leg During Motion," IEEE Trans. Neural Syst. Rehabil. Eng., **12**(2), pp. 157–165.

[16] Fattah, A., and Agrawal, S., 2005, "On the Design of a Passive Orthosis to Gravity Balance Human Legs," ASME J. Mech. Des., **127**(4), pp. 802–808.

[17] Schultz, A. B., Alexander, N. B., and Ashton-Miller, J. A., 1992, "Biomechanical Analysis of Rising from a Chair," J. Biomech., **25**(12), pp. 1383–1391.

[18] NASA Reference Publication 1024, 1978, "Anthropometric Source Book: Volume I: Anthropometry for Designers," NASA.

[19] Riener, R., and Fuhr, T., 1998, "Patient-Driven Control of FES-Supported Standing Up: A Simulation Study," IEEE Trans. Rehabil. Eng., **6**(2), pp. 113–124.

[20] Angeles, J., 1997, *Fundamentals of Robotic Mechanical Systems: Theory, Methods, and Algorithms*, Springer-Verlag, New York.

[21] Goulart, F. R. P., and Valls-Sole, J., 1999, "Patterned Electromyographic Activity in the Sit-to-Stand Movement," Clin. Neurophysiol., **110**, pp. 1634–1640.

[22] Banala, S. K., Agrawal, S. K., Fattah, A., Rudolph, K., and Scholz, J. P., 2004, A Gravity Balancing Leg Orthosis for Robotic Rehabilitation, *Proceedings of the 2004 IEEE International Conference on Robotics and Automation*, pp. 2474–2479, New Orleans, LA.